SKBF
KBS

TEKNISK
RAPPORT

82-10

The hydraulic properties of fracture zones and tracer tests with non-reactive elements in Studsvik

Carl-Erik Klockars
Ove Persson
Geological Survey of Sweden, Uppsala

Ove Landström, Studsvik Energiteknik AB, Nyköping

Sweden, April 1982

SVENSK KÄRNBRÄNSLEFÖRSÖRJNING AB / AVDELNING KBS

POSTADRESS: Box 5864, 102 48 Stockholm, Telefon 08-67 95 40

THE HYDRAULIC PROPERTIES OF FRACTURE ZONES AND TRACER TESTS WITH NON-REACTIVE ELEMENTS IN STUDSVIK

Carl-Eric Klockars
Ove Persson
Geological Survey of Sweden, Uppsala, Sweden
Ove Landström
Studsvik Energiteknik, Nyköping, Sweden
April, 1982

A list of other reports published in this series during 1982, is attached at the end of this report. Information on KBS technical reports from 1977-1978 (TR 121), 1979 (TR 79-28), 1980 (TR 80-26) and 1981 (TR 81-17) is available through SKBF/KBS.

THE HYDRAULIC PROPERTIES OF FRACTURE ZONES AND TRACER TESTS WITH NON-REACTIVE ELEMENTS IN STUDSVIK

Carl-Erik Klockars	Geological Survey of Sweden
Ove Persson	-"-
Ove Landström	Studsvik Energiteknik AB

Uppsala, April 1982

TABLE OF CONTENTS

SUMMARY

Tracer technique was applied in a rock formation within the Studsvik Energiteknik area in order to study hydrodynamic properties of discrete fracture zones between boreholes. The two-hole method was applied in these studies; a nonreactive tracer is injected in one hole into a fracture zone which is in hydraulic contact with a central pump hole (observation hole). Hydraulic tests and TV inspection were carried out in the fracture zones. Chemical composition of the groundwater was determined.

In summary, the following hydraulic properties were found for the fracture zones between the boreholes B1N-B6N and B5N-B6N respectively, under the prevailing conditions:

- The fracture zones studied consist of a number of transport pathways with different mean transit times, varying from 100 to 1200 hours.

- The fracture zone between boreholes B1N and B6N has a mean hydraulic conductivity of $6\text{-}7 \cdot 10^{-5}$ m/s and the fracture zone between boreholes B5N and B6N, $2 \cdot 10^{-4}$ m/s.

- The kinematic porosity of the fracture zones studied, calculated as the ratio between the hydraulic conductivity of the rock mass and that of the fracture zone, is $2 \cdot 10^{-3}$ and $5 \cdot 10^{-3}$, respectively.

- The roughness factor β, which expresses the ratio between measured and theoretically calculated (plane-parallel) fracture conductivity for the fracture zones studied, is approximately 0.04 and 0.06, respectively.

- Dispersivity for the flow channels within the fracture zones is of the order of 0.3-0.8 m.

- The groundwater encountered is a nearly neutral, probably reducing, Na-Ca-HCO_3 water.

The results of the tracer tests reveal the following:

- I-131 is a suitable nonreactive tracer for the test area. A test with simultaneous injection of I-131 and T (tritium) gave comparable breakthrough curves.

- Of the three flow paths investigated by tracer technique, two are suited for further tests with sorbing radionuclides, B1N-B6N and B5N-B6N. The third flow path, B8N-B6N, is not well-defined in relation to overlying fracture zones.

1. INTRODUCTION

The Geological Survey of Sweden (SGU) and Studsvik Energiteknik AB carried out field studies of the migration of radionuclides in natural rock fractures during the years 1977-78 (Landström et al, 1978). The tests were carried out in a rock formation (consisting mainly of granite) within Energiteknik AB's area at Studsvik. Studsvik is situated near the Baltic Sea approximately 90 km south of Stockholm. The work was conducted under contract to PRAV and KBS.

Under contract to PRAV and later KBS, SGU located and prepared a new test site for further migration studies. This site is situated in the northern part of Studsvik where the bedrock consists of a sedimentary gneiss. On the basis of the results of introductory geological and geophysical studies, 8 holes (Ø = 115 mm) were hammer-drilled to a depth of about 100 m (B1N-B8N in fig. 1a). A 200 m core borehole was also drilled (Ø 56 mm) for the determination of rock species, fracture minerals etc. (K1N in fig. 1a).

A series of hydrological, radiometric and geochemical tests and measurements were performed in the boreholes for the purpose of: a) identifying fractures and fracture zones that connect the boreholes, and b) characterizing the natural background radioactivity and the geochemical environment. The results of these studies were reported by Klockars et al (1980) and Landström (1980).

For the purpose of selecting and characterizing fracture zones (flow paths) suitable for coming migration studies, the hydrological investigations were supplemented with pump tests and tracer tests with nonreactive tracers. The results of these tests and different data for existing flow paths along fracture zones are summarized in the present report.

2. CHOICE OF FRACTURE ZONES FOR TRACER TESTS

Fracture zones within the test area were located by means of conventional hydraulic test methods, such as water injection tests and interference tests. These methods, together with test pumping, provided the basis for the choice of the extraction hole (B6N) and three nearby injection boreholes (B1N, B5N and B8N) with fracture zones suitable for tracer tests, see fig. 2a. Methods and results have been described by Klockars et al (1980).

3. GEOMETRIC DATA FOR SELECTED FRACTURE ZONES

Different geophysical borehole methods were used to obtain information on the geometry of the fracture zones. The distance between the sections in boreholes B1N, B5N, B8N and the sections in pumphole B6N between which hydraulic contact is established are shown in the table 3a. They were calculated from the results of deviation measurements and levelling of the boreholes.

Table 3a Distance between contact zones in different boreholes

Injection hole	Section	Pump hole B6N, section	Distance
B1N	91.0 - 92.3 m	94 - 102 m	11.8 m
B5N	78.8 - 80.1 m	64 - 66 m	14.6 m
B8N	76.0 - 77.3 m	64 - 66 m	22.6 m

TV logging of the boreholes revealed the number of fractures as well as the strike and dip of the fractures in the sections in question, see table 3b.

Table 3b Number of fractures in borehole sections and their strike and dip

Borehole	Section	Number of fractures	Strike	Dip
B1N	91.0 - 92.3 m	4	N 35 - 45°W	55 - 75°N
B5N	78.8 - 80.1 m	1	N 5°W	45°N
		6	N 15°W	35 - 55°N
		1	N 25°W	35°N
B6N	64 - 66 m	3	N 30 - 35°W	60 -70°N
		4	N 45 - 60°W	55 - 70°N
		1	N 80°W	75°N
B8N	76.0 - 77.3 m crushed zone			
		1	N 60°W	70°N

4. HYDRAULIC CONDUCTIVITIES FROM HYDRAULIC TESTS

4.1 General

The hydraulic tests included introductory water injection tests and a number of interference tests, described by Klockars et al (1980). On the basis of the results of the interference tests, a test pumping was carried out in borehole B6N. Fracture zones were sealed off with double packers in those boreholes that exhibited good contact with B6N, see table 4.1a. In order to prevent the inward leakage of superficial groundwater during pumping, single packers were installed below fracture zones located near the surface, see table 4.1a.

Table 4.1a Location of the packers in the boreholes

Borehole	Packer level	
	Single	Double
B1N		91.0 - 92.3 m
B5N	30 m	78.8 - 80.1 m
B6N	30 m	
B8N	28 m	76.0 - 77.3 m

4.2 Hydraulic conductivity

By "hydraulic conductivity" is meant the quantity of water per unit time that passes through a unit area of a cross-section of the water-bearing medium perpendicular to the flow direction over a unit gradient and at a given water temperature.

The hydraulic conductivity, k_p, of the selected fracture zones was calculated from the results of water injection tests, interference tests, test pumping and slug tests, Klockars et al (1980). The results are summarized in table 4.2a.

Table 4.2a Hydraulic conductivity, k_p for selected borehole sections calculated by means of different methods.

Borehole	Section	Water injection test	Interference test	Test pumping	Slug test
B1N	91.0-92.3 m	$1.7 \cdot 10^{-7}$ m/s		$8.5 \cdot 10^{-7}$ m/s	$1 \cdot 10^{-6}$ m/s
B5N	78.8-80.1 m	$5.1 \cdot 10^{-7}$ m/s	$2 \cdot 10^{-6}$ m/s	$2.5 \cdot 10^{-6}$ m/s	$6 \cdot 10^{-6}$ m/s
B6N	30-102 m	$3.1 \cdot 10^{-7}$ m/s		$2.4 \cdot 10^{-6}$ m/s	
B8N	76.0-77.3 m	$9.1 \cdot 10^{-8}$ m/s	$2 \cdot 10^{-6}$ m/s	$2.6 \cdot 10^{-6}$ m/s	$6 \cdot 10^{-6}$ m/s

The hydraulic conductivity values from the different methods (table 4.2a) are not directly comparable, since the length of the measurement section varied. The packer distance in water injection tests and interference tests was 2 m, while in test pumping and slug tests it was 1.3 m.

Interference tests and test pumpings are based on the same principle and exhibit similar results. The lowest hydraulic conductivities were obtained with the water injection method. The slug tests give the highest conductivity values, but are, like the water injection tests, only valid in the immediate vicinity of the boreholes. The interference tests and test pumpings, on the other hand, give a mean value for the hydraulic conductivity between pump hole B6N and the different observation holes (B1N, B5N and B8N).

No drawdown above the single packers or in boreholes B2N, B3N or B4N was recorded during the test pumping period. This indicates that the superficial groundwater was kept out of the deeper-lying zones. This is also indicated by the groundwater chemistry of pumped water from B6N, which is characteristic of groundwater from deeper zones, see section 5.2.

In the test pumping procedure, the entire borehole B6N below the single packer was pumped. The pump capacity, which was kept constant during pumping, was equal to the total flow from the different fracture zones to the pump well. The hydraulic conductivity of individual fracture zones (table 4.2a) was calculated from this total flow, resulting in a higher value than if the test pumping had been performed only in the fracture zone.

Hydraulic conductivity was calculated from the test pumping data in accordance with equations (1) and (2), assuming radial flow in a homogeneous porous medium.

$$T = \frac{Q}{4\pi s} W(u) \qquad (1)$$

where T = transmissivity $\left[m^2/s\right]$
Q = pump capacity $\left[m^3/s\right]$
s = drawdown $[m]$
$W(u)$ = Theiś well function

$$T \cong \Sigma Lk_p \qquad (2)$$

where L = length of measurement section $[m]$
k_p = hydraulic conductivity of measurement section $[m/s]$

ΣLk_p can be calculated for the pump hole from water injection measurements. There are three fracture zones in pump hole B6N below the single packer at the 30 m level (Klockars et al, 1980). These three fracture zones account for the main portion (93%) of ΣLk_p and thereby give most of the flow to the pump well. Since the flow to the borehole from a fracture zone is proportional to Lk_p, the portion of the pump flow coming from each fracture zone, α , can be calculated, see table 4.2b.

Table 4.2b Major fracture zones in B6N and their percentage contribution to the pump flow in B6N

Level	Portion of flow (α)
38- 40	15%
64- 66	70%
94-102	8%

On the basis of the calculated contribution to total pump flow from each fracture zone in B6N, α , the hydraulic conductivity of the different fracture zones was calculated from test pumping data in accordance with equation (3) and is presented in table 4.2c.

$$k_{pk} = \alpha \cdot \frac{T}{L} \qquad (3)$$

where T = transmissivity of observation section $\left[m^2/s\right]$

L = section length in observation hole $\left[m\right]$

Table 4.2c The hydraulic conductivity, k_{pk}, of selected fracture zones calculated from test pumping data with corrected flow

Fracture zone	k_{pk} [m/s]
B1N:91.0 - 92.3 m --- B6N:94 - 102 m	$6.8 \cdot 10^{-8}$ m/s
B5N:78.8 - 80.1 m --- B6N:64 - 66 m	$1.7 \cdot 10^{-6}$ m/s
B8N:76.0 - 77.3 m --- B6N:64 - 66 m	$1.8 \cdot 10^{-6}$ m/s

5. GROUNDWATER CONDITIONS

5.1 Groundwater level observations

Packers were placed in existing boreholes as shown in table 4.1a. The groundwater levels were recorded at different times in the sections between the packers. This level has been assumed to represent the groundwater head in the fracture zones within a particular section. Figure 5.1a shows that the groundwater heads in the different fracture zones react similarly during the observation period. The fracture zones in boreholes B5N and B8N have about 2-3 m higher piezometric heads than the fracture zones in B1N and the pump well B6N.

The recorded levels follow each other well during the period from June to October. On the 7th of October, continuous injection of groundwater began in borehole B1N. In the injection zone in B1N, the level rose about 3 m relative to the pump well, see fig. 5.1a. The elevated level of the groundwater in B1N then persisted. During the latter part of March, the groundwater head rose sharply; after about one week, the head had increased from 21 m to 23 m, and after another week to 29 m. Injection of groundwater was interrupted on the 25th of March as a steady-state condition had not been achieved. The cause of the level change is probably a reduction of hydraulic conductivity in the injection zone in B1N.

Slug tests performed prior to water injection gave conductivity values of $1 \cdot 10^{-6}$ m/s for the injection zone. Similar measurements after the conclusion of injection gave a conductivity of $1 \cdot 10^{-7}$/s. The change is assumed to be due to clogging as a result of the fact that the injected groundwater is oxygenated, affecting dissolved ions in the originally reducing conditions in the injection zone and causing them to precipitate.

5.2 Chemical conditions

The chemical composition of the groundwater and its variation with time are shown in table 5.2a, which presents the results of analyses of water pumped up from the pump hole, B6N. Air in contact with the water samples during sampling, could have had some effect on their chemistry. The reported pH values were determined in connection with sampling other values in the laboratory. The water samples were kept frozen between sampling and analysis.

The temperature of the pumped-up water (see fig. 5.2a) indicates that this water (or most of it) probably originates from a depth of the order of 200 m, on the basis of the measured temperature gradient, Landström (1980). Preliminary measurements of the redox potential of the pumped-up water indicate reducing conditions.

Upon failure of a packer in borehole B1N (80-12-07), superficial water entered the system, which is shown by the conductivity-time curve in fig. 5.2a and by the analysis "80-12-10" in table 5.2a, which is characterized by, among other things, a reduced concentration of cations and an increased concentration of NO_3. As is evident from the conductivity curve, equilibrium is quickly restored.

Table 5.2a Analysis of pumped-up water from B6N

			80-06-16	80-07-09	80-19-17	80-10-28	80-12-10	80-12-29	81-02-24
Spec. conductivity,		µS/cm	300	300	330	350	245	360	380
pH			7.2	6.6	6.5	6.7	6.4	6.4	7.0
$KMnO_4$ demand		mg/l	20	23	26	27	32	33	28
Total hardness,	Ca	"	46	44	49	54	38	57	65
Calcium	Ca	"	31	34	30	34	26	37	44
Magnesium	Mg	"	9	7	12	12	8	12	13
Sodium	Na	"	39	40	43	43	26	45	39
Potassium	K	"	2.8	2.9	2.9	3.7	2.4	2.8	2.9
Chloride	Cl	mg/l	12	11	12	12	10	12	12
Sulphate	SO_4	"	29	29	29	30	34	29	26
Bicarbonate	HCO_3	"	195	200	218	230	133	227	256
Ammonium	NH_4	"	0.04	0.04	0.04	0.05	0.01	0.01	0.02
Nitrite	NO_2	"	<0.01	<0.01	<0.01	<0.01	<0.01	<0.01	<0.01
Nitrate	NO_3	"	0.03	0.04	0.03	0.03	0.39	0.01	<0.01
Phosphate	PO_4	"	0.02	0.01	0.01	0.01	0.01	0.01	0.01
Iron	Fe (II)	"	0.07	0.04	0.04	0.04	0.05	0.09	0.05
Iron	Fe(tot)	"	0.07	0.06	0.07	0.07	0.18	0.11	0.15
Manganese	Mn	"	0.28	0.29	0.30	0.33	0.10	0.36	0.41
Fluoride	F	"	0.30	0.26	0.22	0.23	0.12	0.24	0.27
Silicic acid	SiO_2	"	11	11	12	11	10	11	11
Tot.org.carbon	C	"	4.6	4.7	4.8	5.4	14.9	14.3	6.6

6. TESTS WITH NONREACTIVE TRACERS

6.1 Method and tracers used

The selected fracture zones were utilized to study the transport of different nonreactive water-soluble tracers with the groundwater. The purpose was to characterize the properties, hydraulic conductivity and dispersivity of the medium (the fractures) on the basis of breakthrough curves.

The tests were carried out under controlled conditions. Groundwater was continuously pumped away (with a constant capacity) from borehole B6N. As a result of this, the groundwater flow along the fracture zones listed in table 3.a was directed towards borehole B6N. Tracers were then injected in one of the other boreholes, within the selected fracture zones. The concentration of the tracer in the pumped water was recorded as a function of time after injection. The tests were carried out using the same procedure as that described by Gustafsson and Klockars (1981).

Br-82 (as NH_4Br) was tried in the first experiments but its half-life (36 h) turned out to be too short for the recording of the entire breakthrough curve. Instead, I-131 (as NAI) with a half-life of 8 days was used as a nonreactive tracer in the following experiments. Approximately 10 m Ci was injected in each test. In one experiment 10 m Ci of H-3 (as tritiated water) was injected simultaneously with I-131.

Instantaneous injection means that the tracer solution must be injected into the formation as a point in time and space. The Br-82 injection technique (pumping down the 0.5 l tracer solution through a small-bore hose to the injection zone followed by 20 litres of groundwater, produced unacceptable disturbance of the groundwater flow pattern and the following improved injection technique was devised. In this was considered the requirement that the tracer solution must penetrate out into the water bearing fractures with a minimum of flow pattern disturbance.

The injection of the tracer solution is preceded by one week's injection of groundwater, with the addition of iodide carrier, at a concentration of 0.08 M, during the day before and after the radiotracer injection. The flow is kept low, about 10 ml/min, in order to avoid affecting the flow pattern. The I-131 tracer solution (500 ml with carriers added) is then injected with the same capacity as the preceding groundwater injection. This means that the tracer injection will take a rather long time, about 50 minutes. After the radiotracer injection the groundwater injection is continued in order to drive the tracer solution out into the transport channels of the fracture zone.

6.2 Measurement technique

Br-82 and I-131 in water samples from pump hole B6N were analysed in the laboratory using gamma ray spectrometry. Analyses of H-3 were performed using a liquid scintillation counter. The water samples normally consisted of 0.5 l, but were made larger in a later phase in order to improve the accuracy of the measurements. The samples were collected with the aid of an automatic sampler.

6.3 Presentation of results

The tracer tests called A, B, C and D are presented in table 6.3a.

Table 6.3a Tracer tests

Run	Flow path	Tracer
A	B1N-B6N	I-131
B	B1N-B6N	I-131+T
C	B5N-B6N	I-131
D	B8N-B6N	I-131

The results of the tracer tests are presented in figs. 6.3a-e in the form of breakthrough curves obtained in borehole B6N. Time after injection is plotted on the horizontal axis and recorded concentration in the pump water (C) related to injection concentration (C_o) on the vertical axis. Recovery of tracer is shown in figs. 6.3f-i. Time after injection is plotted on the horizontal axis and cumulutative detected quantity, related to injected quantity, on the vertical axis.

6.4 Dispersivity and transit times

For a two-hole test with instantaneous injection, the concentration of tracer in the pumped-up water as a function of time t and distance x (between injection hole and pump hole) can be calculated with good approximation in accordance with equation (4), which applies to one- dimensional flow (Zuber, 1974).

$$C\ (x,\ t) = \frac{m}{V} \cdot \frac{1}{\sqrt{4 \cdot \pi \cdot \frac{D}{vx} \cdot (\frac{t}{t_o})^3}} \cdot \exp \frac{-(1-\frac{t}{t_o})^2}{4 \cdot \frac{D}{vx} \cdot \frac{t}{t_o}} \quad (4)$$

where t_o = mean transit time

$\frac{D}{vx}$ = dimensionless dispersion parameter where D = dispersion coefficient, v = velocity and x = transport distance

m = total mass (activity) injected

V = total volume of the water-saturated pores in which the water movements take place

According to Kreft et al (1974), V in equation (4) is equal to the water volume obtained during the time t_o and at a pump capacity of Q or

$$V = Q \cdot t_o \qquad (5)$$

Velocity in the case of radial flow is not constant, so equation (4) is only valid for pure mechanical dispersion where the dispersivity D/v can be assumed to be constant and molecular diffusion can be neglected (Zuber, 1974). A premise for the model is that no reactions or other retarding processes take place when the tracer comes into contact with the solid medium (rock mass, fracture minerals etc.).

By fitting theoretically calculated breakthrough curves for instantaneous tracer injection to corresponding experimental breakthrough curves, the mean transit time, t_o, and the dimensionless dispersion parameter $D/_{vx}$ are obtained.

Macrodispersion phenomena can occur in connection with the transport of water-soluble substances in anisotropic media. This is caused by the fact that the transport of tracer from the injection point to the detection point takes place in a number of fractures or channels with different transit times. In such cases, the breakthrough curve is made up of a number of partially superimposed partial curves and extends over a longer period of time than if the transport had taken place in a homogeneous isotropic medium.

Total curves, made up of a number of partial curves calculated according to equation (4), were fitted to the experimentally determined breakthrough curves for tracer tests along the fracture zones B1N-B6N and B5N-B6N. The partial curves were normalized by means of the ratio $\frac{m}{V} \cdot R_i$, where R_i represents the partial curve's share of the total amount of tracer pumped up.

The experimental breakthrough curves can be fitted to the theoretical breakthrough curves in such a manner that several solutions of t_o and $D/_{vx}$ are obtained. The first part of the breakthrough curve has only one fit, however. The subsequent partial curves, which

constitute the difference between the theoretical and the experimental curve, can be fitted in a number of ways, and after the procedure has been repeated to 3-5 partial curves, the parameter fit is almost arbitrary.

Figures 6.4a-f show theoretically calculated partial curves and total curves and comparisons with experimental data for tracer tests B and C in fracture zones B1N-B6N and B5N-B6N.

Tables 6.4a-b give the mean transit time, t_o, for several fits for tests with injection of I-131 in B1N and B5N. Tables 6.4c-d give corresponding values for the dispersion parameter D/v (dispersivity). The correlation between dispersivity and Peclet's number is given by the following equation:

$$Pe = \frac{1}{D/vx} \qquad (6)$$

where Pe = Peclet's number
D/v = dispersivity
x = distance in metres between injection and observation holes

Table 6.4a Mean transit time t_o for theoretical partial curves in 4 fitting attempts to the breakthrough curve for test B (simultaneous injection of I-131 and T in borehole B1N)

Fitting attempt	Mean transit time t_o [h], for partial curve: I	II	III
B_1	288	490	900
B_2	288	500	900
B_3	285	490	950
B_4	285	500	1000

Table 6.4b Mean transit time t_o for theoretical partial curves in 2 fitting attempts to the breakthrough curve for test C (injection of I-131 in borehole B5N).

Fitting attempt	Mean transit time t_o [h], for partial curve: I	II	III	IV	V	VI	VII	VIII
C_1	85	154	230	330	430	630	800	1100
C_2	84	133	200	290	400	600	800	1200

Table 6.4c Dispersivity D/v for theoretical partial curves in 4 fitting attempts to the breakthrough curve for test B (simultaneous injection of I-131 and T in borehole B1N)

Fitting attempt	Dispersivity D/v [m], for partial curve: I	II	III
B_1	0.39	0.39	0.39
B_2	0.30	0.47	0.59
B_3	0.36	0.53	0.71
B_4	0.36	0.59	0.83

Table 6.4d Dispersivity D/v for theoretical partial curves in 2 fitting attempts to the breakthrough curve for test C (injection of I-131 in borehole B5N)

Fitting attempt	Dispersivity D/v [m], for partial curve: I	II	III	IV	V	VI	VII	VIII
C_1	0.58	0.58	0.58	0.58	0.58	0.58	0.58	0.58
C_2	0.29	0.36	0.39	0.44	0.51	0.58	0.60	0.73

The dispersivity D/v has the greatest range of variation, a factor of 2-3, while the mean transit time t_o varies by about 10% between different fits. The dispersivity D/v increases with the mean transit time. In tracer tests carried out in the Finnsjö area, D/v was found to be constant for the partial curves and was therefore interpreted as a material constant, in analogy with porous homogeneous media, Gustafsson and Klockars (1981). The results obtained here can be interpreted as indicating that a limit has been reached for the validity of the assumptions made, i.e. the theoretical premises probably do not apply or the tested flow paths are much too complex. The transit times are on the order of a power of 10 longer than in the Finnsjö area, which means that the premise of the model that diffusion can be neglected is probably not met.

By calculating the portion of tracer that has been transported along the different transport pathways of the total curve, a weighted average transit time, $\bar{t}_o$, has been calculated for the fracture zone as follows:

$$\bar{t}_o = \Sigma \; t_{oi} \cdot R_i \qquad (7)$$

where $\bar{t}_o$ = weighted average transit time for total curve
t_{oi} = partial curve's mean transit time
R_i = partial curve's portion of pumped-up quantity of tracer of total curve

Table 6.4e The weighted average transit time in 4 fitting attempts for test B (simultaneous injection of I-131 and T in the fracture zone between B1N and B6N)

Fitting attempt	Mean transit time $\bar{t}_o$ [h]
B_1	508
B_2	512
B_3	530
B_4	547

Table 6.4f The weighted average transit time in 2 fitting attempts for test C (injection of I-131 in the fracture zone between B5N and B6N)

Fitting attempt	Mean transit time $\bar{t}_o$ [h]
C_1	389
C_2	410

6.5 Hydraulic fracture conductivity and kinematic porosity

The average hydraulic conductivity of the tested fracture zone has been calculated from the resultant total curves with the assumption of stationary two-dimensional radially symmetric laminar flow in accordance with:

$$k_e = \frac{\ln (r_b/r_a)}{2\,\bar{t}_o} \cdot \frac{r_b^2 - r_a^2}{\Delta h} \qquad (8)$$

where k_e = hydraulic conductivity [m/s]
r_b = distance between injection hole and detection hole [m]
r_a = radius of pump hole [m]
$\bar{t}_o$ = weighted mean transit time [s]
Δh = difference in pressure head between injection hole and pump hole [m w.g.]

The difference in pressure head, Δh, between the injection hole and the pump hole was measured during the tracer test, see table 6.5a.

Table 6.5a Difference in pressure head, Δ h, between injection hole and pump hole at the times of the different tests

Test	Flow path	Δh [m]
A	B1N-B6N	3.0
B	B1N-B6N	3.0
C	B5N-B6N	2.5
D	B8N-B6N	2.5

Average hydraulic fracture conductivity values for fracture zones B1N-B6N and B5N-B6N are presented in tables 6.5b and 6.5c.

Table 6.5b The weighted average hydraulic fracture conductivity determined in connection with 4 fitting attempts to the breakthrough curve in test B (simultaneous injection of I-131 and T in borehole B1N)

Fitting attempt	$\bar{k}_e$ [m/s]
B_1	$6.8 \cdot 10^{-5}$
B_2	$6.8 \cdot 10^{-5}$
B_3	$6.5 \cdot 10^{-5}$
B_4	$6.4 \cdot 10^{-5}$

Table 6.5c The weighted average hydraulic fracture conductivity determined in connection with 2 fitting attempts to the breakthrough curve in test C (injection of I-131 in borehole B5N)

Fitting attempt	$\bar{k}_e$ [m/s]
C_1	$1.7 \cdot 10^{-4}$
C_2	$1.6 \cdot 10^{-4}$

An equivalent fracture conductivity was calculated from the water injection data as follows:

$$k_j = \sqrt[3]{\frac{L^2 \cdot k_p^2 \cdot g}{n^2 \cdot 12 \cdot \nu}} \qquad (9)$$

where k_j = hydraulic conductivity for a plane-parallel fracture with laminar flow $\left[m/s\right]$
L = length of measurement section $\left[m\right]$
k_p = hydraulic conductivity of measurement section $\left[m/s\right]$
g = acceleration due to gravity $\left[m/s^2\right]$
n = number of fractures
ν = kinematic viscosity $\left[m^2/s\right]$

The mean, $\bar{k}_p$, of the values of the hydraulic conductivity of the measurement section, which were determined in the injection hole and the pump hole, was inserted in equation (9). The number of fractures, n, or channels in which water flows through the fracture zone between the boreholes was obtained by interpretation of the breakthrough curves. All fractures within one measurement section were assumed to have the same width. Table 6.5d gives $\bar{k}_p$ and k_j as well as k_{pk}, which is the corrected hydraulic conductivity determined from test pumping data, see chapter 4.2.

Table 6.5d Hydraulic mean conductivity in measurement section measured by means of the water injection method, $\bar{k}_p$, and corresponding equivalent fracture conductivity k_j as well as corrected hydraulic conductivity from test pumping data, k_{pk}

Fracture zone	$\bar{k}_p\left[m/s\right]$	$k_j\left[m/s\right]$	$k_{pk}\left[m/s\right]$
B1N-B6N	$1.4 \cdot 10^{-7}$	$1.7 \cdot 10^{-3}$	$6.8 \cdot 10^{-8}$
B5N-B6N	$7.6 \cdot 10^{-7}$	$2.7 \cdot 10^{-3}$	$1.7 \cdot 10^{-6}$
B8N-B6N	$5.5 \cdot 10^{-7}$		$1.8 \cdot 10^{-6}$

The flow in naturally occurring fractures cannot be regarded as plane-parallel owing to the irregularity and roughness of the fracture faces. This means that the calculated equivalent fracture conductivity, k_j, will deviate from the measured hydraulic conductivity, k_e, for the fracture zone by a factor β ("roughness factor") in accordance with the following equation:

$$k_e = \beta \cdot k_j \qquad (10)$$

The ratio between the measured hydraulic conductivity of the rock mass, k_p, and the conductivity of the fractures, k_e, constitutes the ratio between the gross velocity of the water and velocity in the individual fracture, provided that Darcy's law applies and that the gradient is the same over the rock mass as over the fracture. This ratio is called the kinematic porosity, θ_k, and strictly expresses the portion of the rock mass available for water transport.

$$\theta_k = \frac{k_p}{k_e} \qquad (11)$$

Calculated values of the kinematic porosity, θ_k, and the roughness factor, β, are presented in table 6.5e. The variation intervals for the parameters obtained from evaluation of the breakthrough curves are given in the table.

Table 6.5e Values obtained for kinematic porosity, θ_k, and roughness factor, β, determined from total curve

Test	Flow path	θ_k	β
B	B1N-B6N	$2.1\text{-}2.2 \cdot 10^{-3}$	$3.7\text{-}4.0 \cdot 10^{-2}$
C	B5N-B6N	$4.5\text{-}4.7 \cdot 10^{-3}$	$6.1\text{-}6.3 \cdot 10^{-2}$

7. CONCLUSIONS

Tracer tests were carried out in previously investigated fracture zones within the test area at Studsvik. Together with the results of hydraulic tests and geophysical borehole investigations, these tests have provided information on the hydraulic and, to some extent, geometric characteristics of the fracture zones.

I-131 was used as a nonreactive (non-interacting) tracer in the tests. The choice of tracer element was mainly determined by previous experience and suitable half-life. The injection of carrier in the form of non-radioactive iodine preceded each test. A modified pulse injection technique was used in order to avoid disturbing the flow between the boreholes while simultaneously ensuring that the tracer solution actually penetrates out into the water-bearing channels.

The simultaneous injection of T (tritium) and I-131 was tried. No significant difference was obtained between the breakthrough curves of the two elements, which verifies the suitability of iodine as a nonreactive tracer.

A simplified analytical model involving one-dimensional flow of nonreactive tracers between two boreholes was used as a basis for determining dispersivity and mean transit time. Parameters were determined in two attempts by means of a curve fitting technique with good detail resolution. The model gives similar results by assuming that the flow in the fracture zones between the boreholes takes place along a number of flow paths. This is shown by the fact that the theoretical curve consists of a number of partially superimposed partial curves. TV logging also revealed a number of fractures in tested sections.

Since velocity is not constant in the case of radial flow, the model is based on the premise that diffusion can be ignored. This is not likely to be the case at the transit times that apply for the tests carried out here. This is indicated chiefly by the fact that theoretical curves with several parameter compositions can be fitted to the experimentally obtained breakthrough curves.

This means that dispersivity has different values for different fits, with a tendency towards increasing dispersivity with increasing mean transit time for constituent partial curves. For determining hydraulic fracture conductivity and thereby kinematic porosity, however, the simplified analytical model seems to yield credible values.

8. LITERATURE REFERENCES

CARLSSON, L., Gidlund, G., HANSSON, K. and KLOCKARS, C-E. 1979: Estimation of hydraulic conductivity in Swedish Precambrian crystalline bedrock. OECD - NEA, Workshop Mars 1979, Paris.

GIDLUND, G., HANSSON, K. and THOREGREN, U. 1979: Kompletterande permeabilitetsmätningar i Karlshamnsområdet. KBS, Technical Report, No. 79-06, Stockholm.

GUSTAFSSON, E. and KLOCKARS, C-E. 1981 Studies on groundwater transport in fractured crystalline rock under controlled conditions using non-radioactive tracers. KBS, Technical Report, No 81-07.

KLOCKARS, C-E., PERSSON, O., CARLSSON, L., DURAN, O., LINDSTRÖM, D., MAGNUSSON, K-Å and SCHERMAN, S. 1980: Preparatory hydrogeologic investigations for in situ migration experiments in Studsvik. Report Prav 4.17.

KREFT, A., LENDA, A., TUREK, B., ZUBER, A. and CZAUDERNA, K. 1974: Determination of effective porosites by the two-well pulse method. Isotope Techniques in Groundwater Hydrology 1974. (Proc. Symp. Vienna, 1974), IAEA, Vienna.

LANDSTRÖM, O. 1980: Preparatory work on in situ migration experiments in Studsvik. Report Prav 4.18.

LANDSTRÖM, O., KLOCKARS, C-E., HOLMBERG, K-E and WESTERBERG, S. 1978: In situ experiments on nuclide migration in fractured crystalline rocks. KBS Teknisk rapport 110, Stockholm.

LENDA, A. and ZUBER, A. 1970: Tracer disperson in groundwater experiments. Proceedings of a symposium arranged by IAEA, Vienna.

SNOW, D.T. 1968: Rock fracture spacings, openings and porosities, J. Soil Mech. Found. Div. Prov. ASCE, Vol. 94 No SM 1.

ZUBER, A. 1974: "Theoretical possibilities of the two-well pulse method", Isotope Techniques in Groundwater Hydrology 1974 (Proc. Symp. Vienna, 1974), IAEA, Vienna.

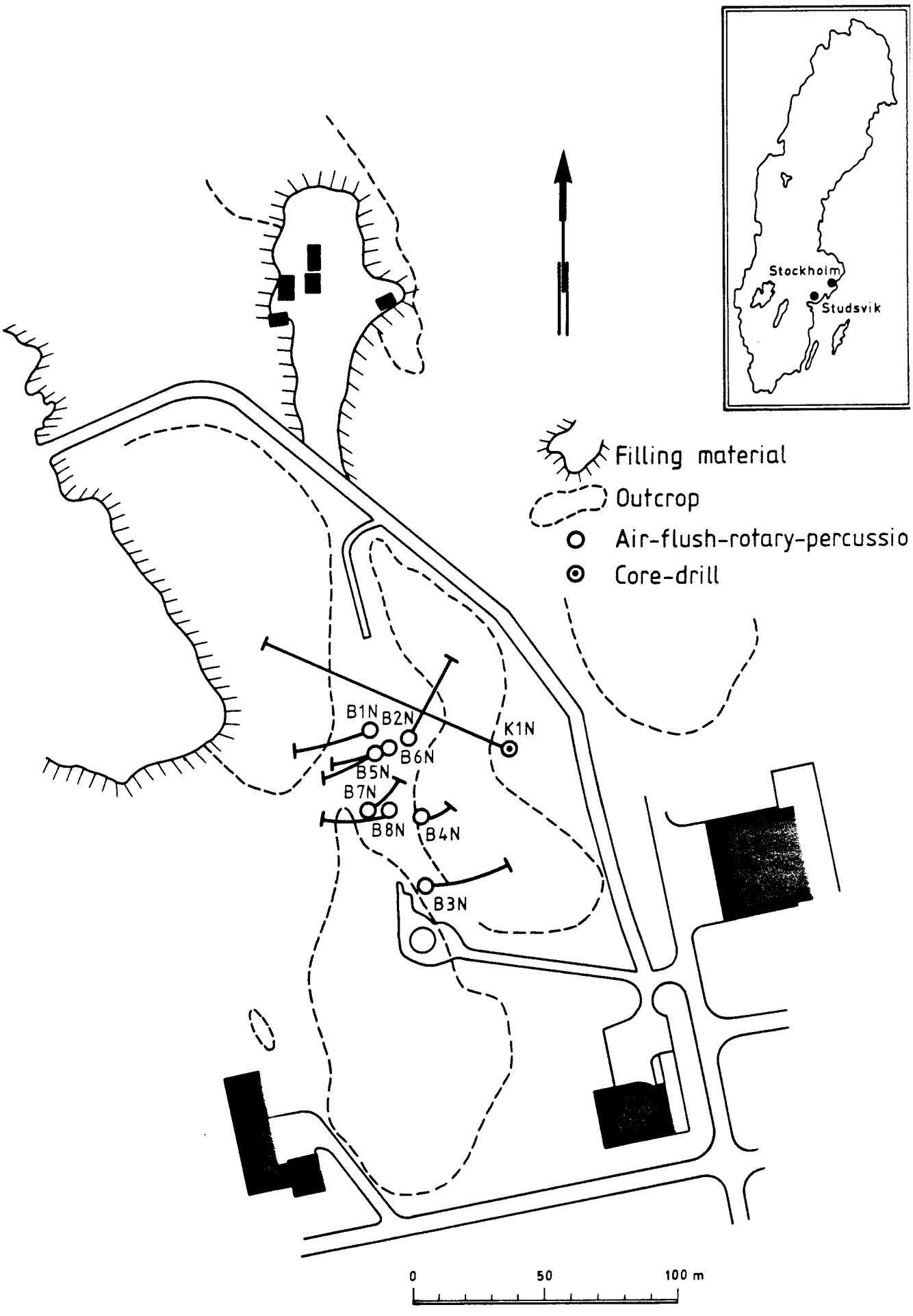

Fig. 1a Location of the boreholes and their projection onto the horizontal plane.

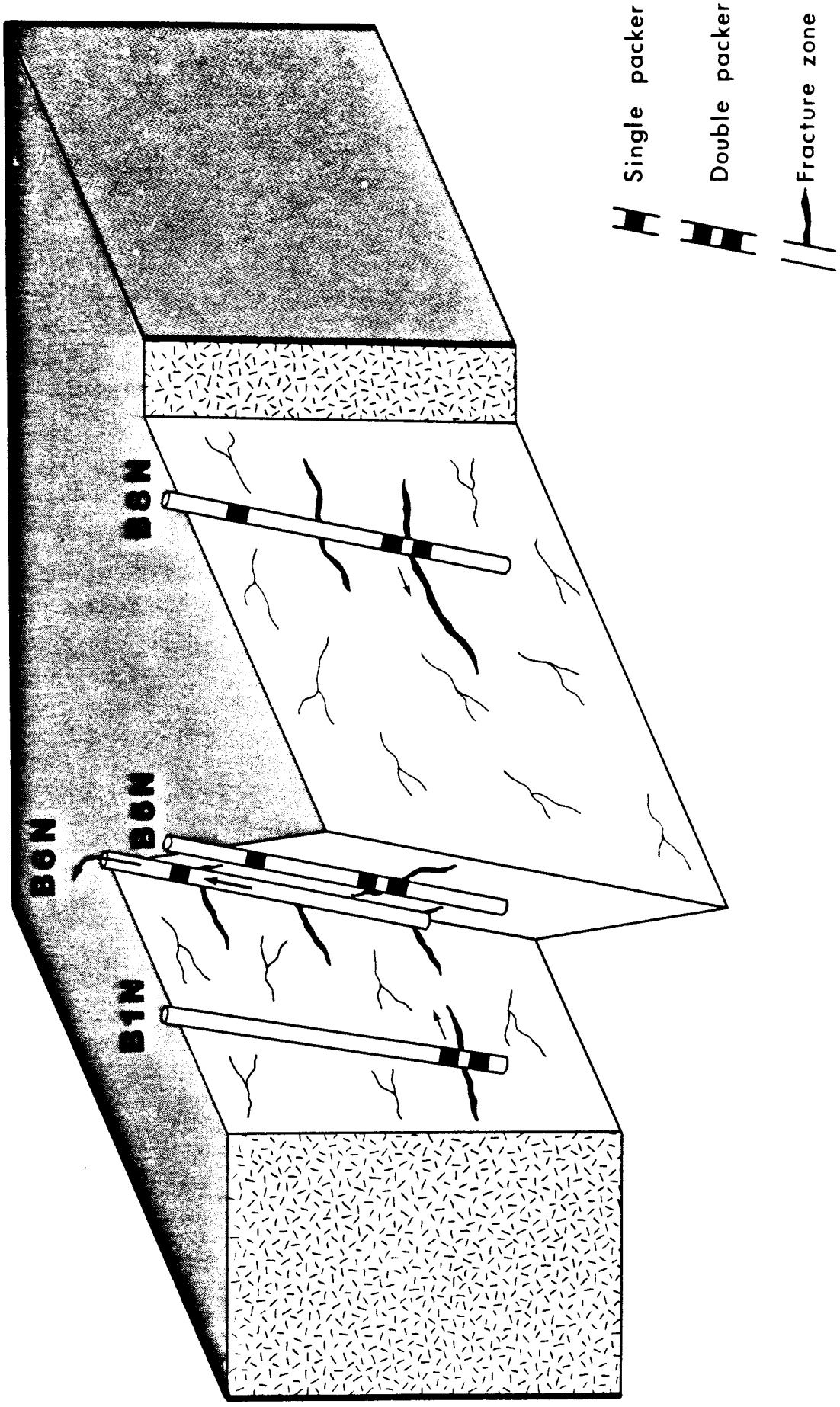

Fig. 2A Cutaway view of test site showing pump hole (B6N) and injection holes with discrete fracture zones (B1N, B5N and B8N).

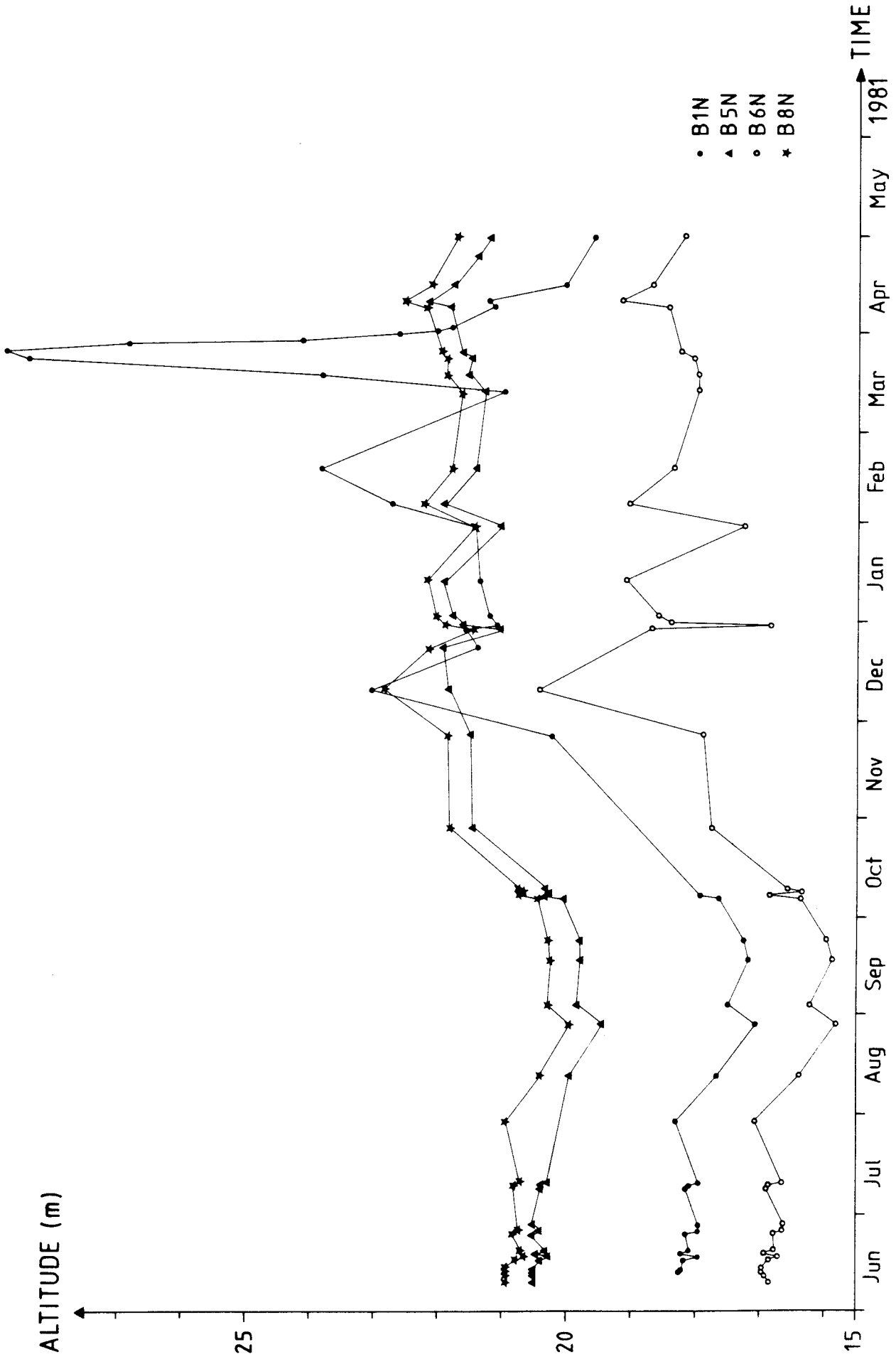

Fig. 5.1a Variation of groundwater level with time in the shielded sections.

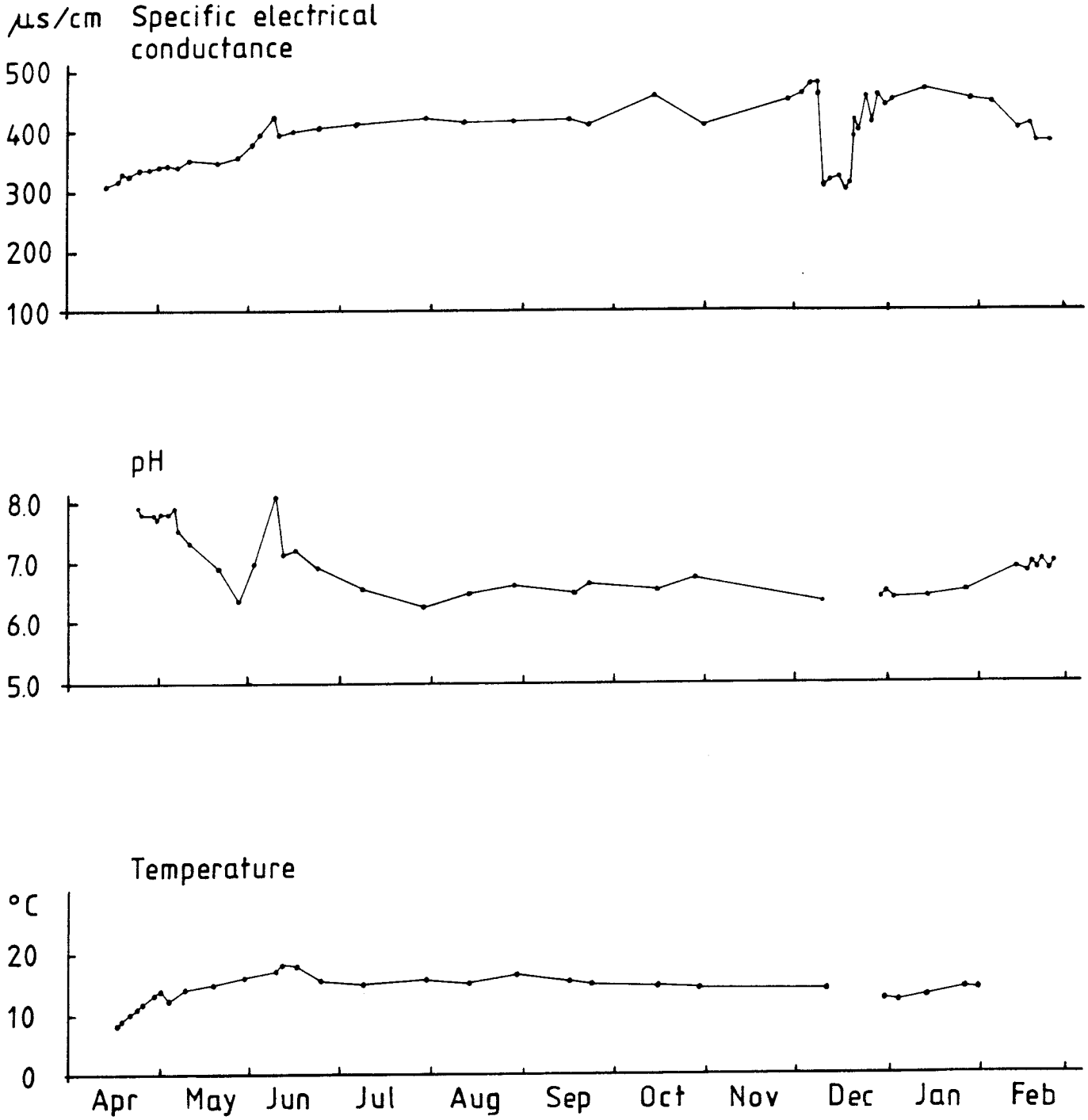

Fig. 5.2a Specific electric conductance, pH and temperature in water pumped up from B6N.

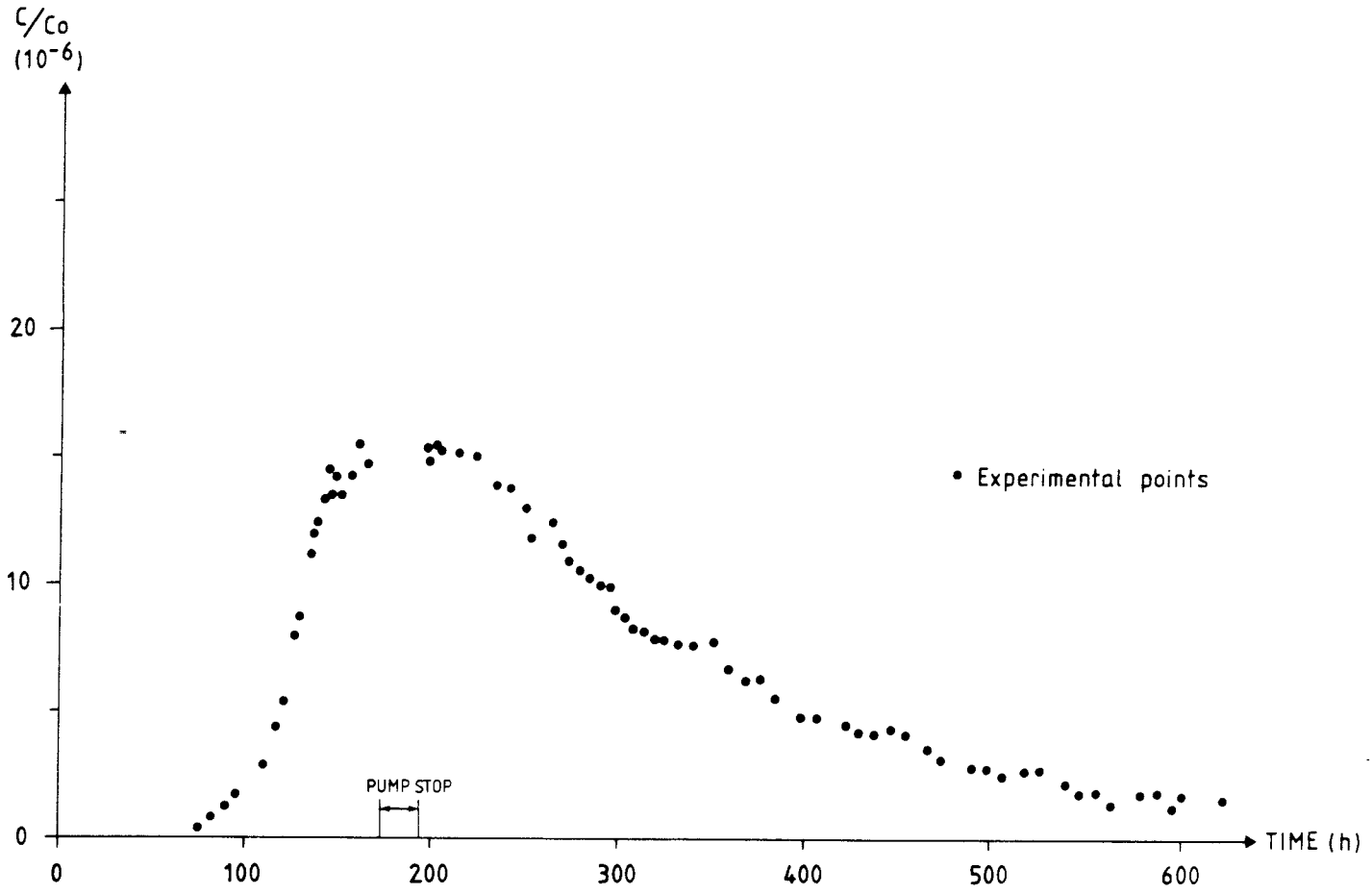

Fig. 6.3a Breakthrough curve for I-131 in test A.

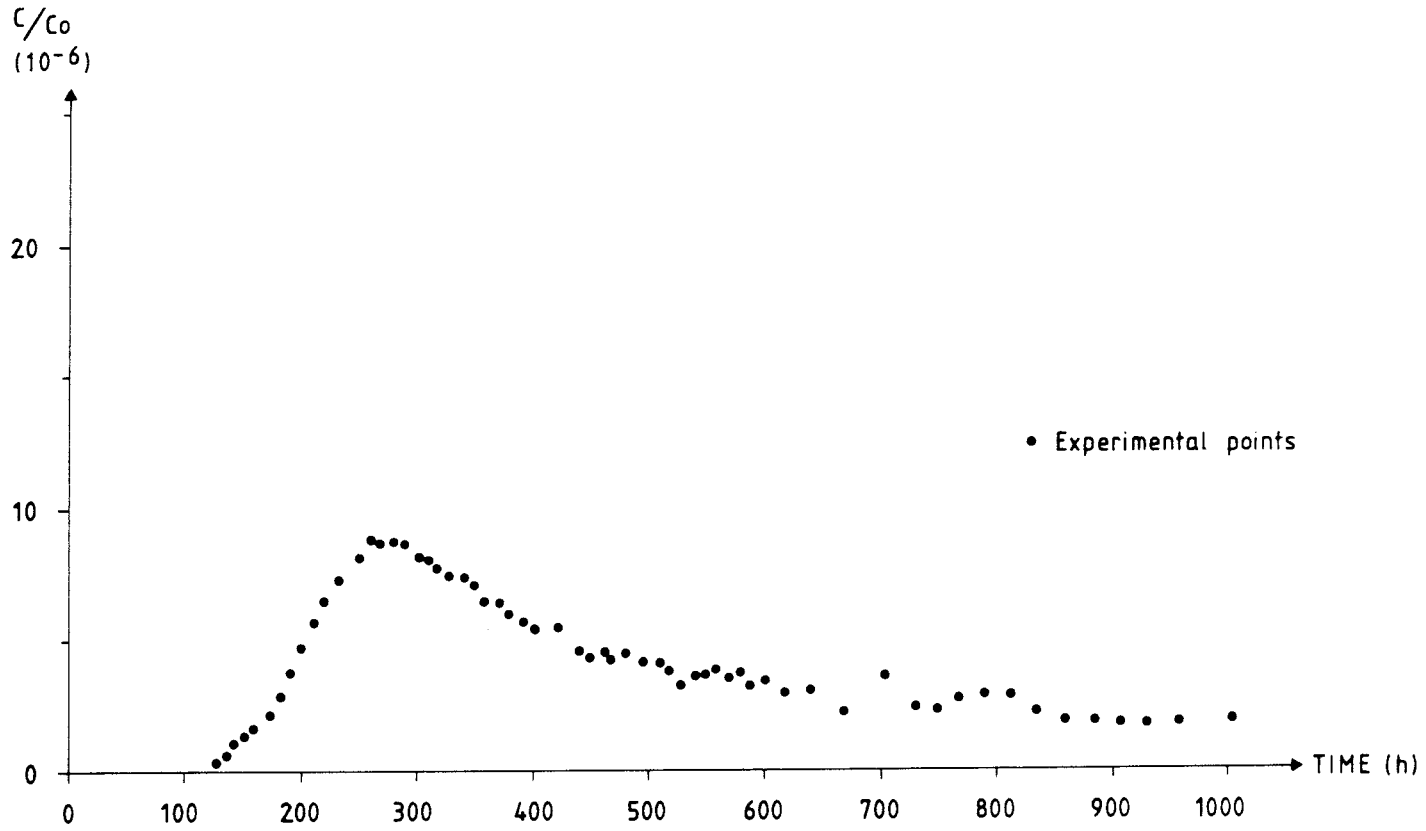

Fig. 6.3b Breakthrough curve for I-131 in test B.

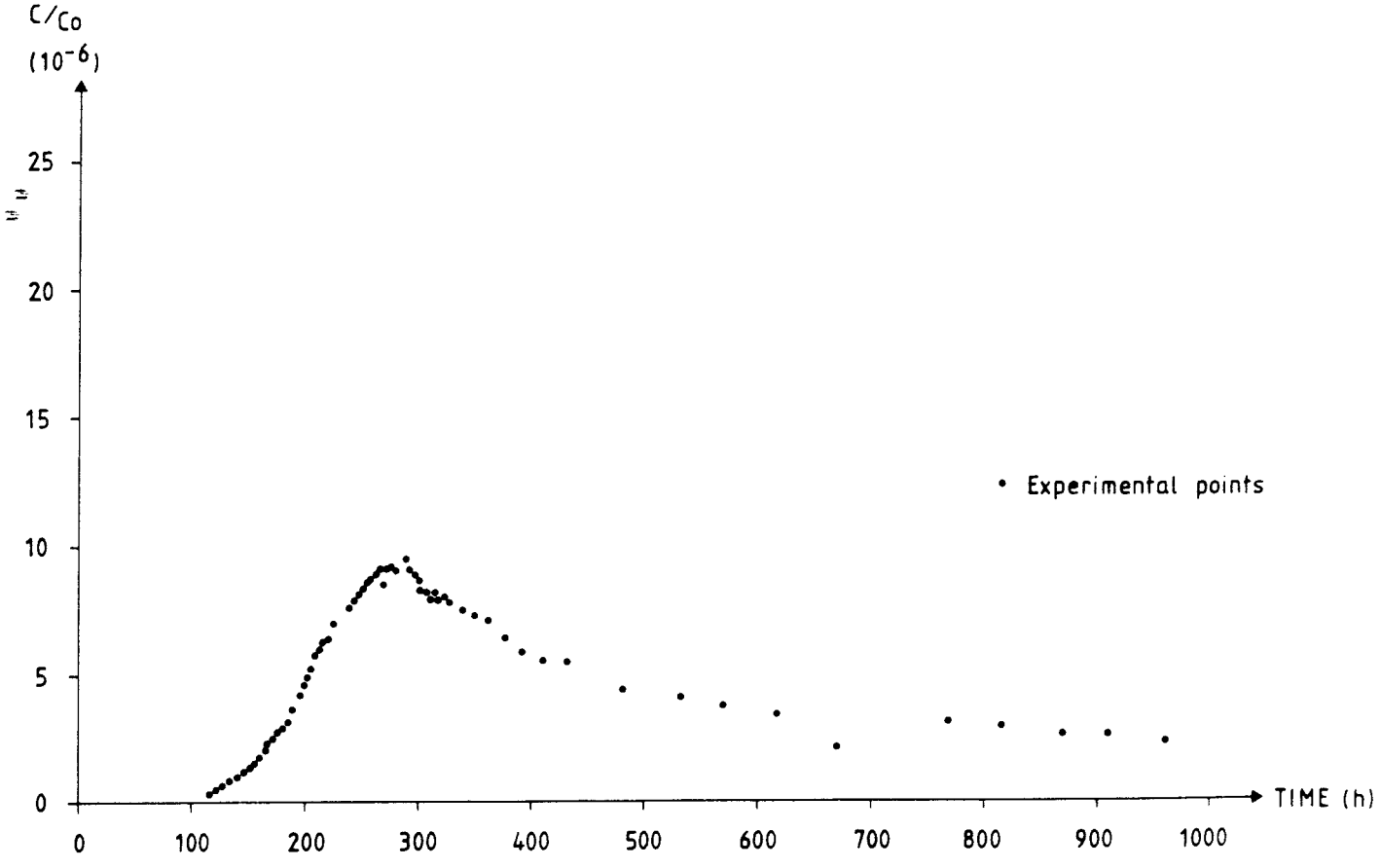

Fig. 6.3c Breakthrough curve for T in test B.

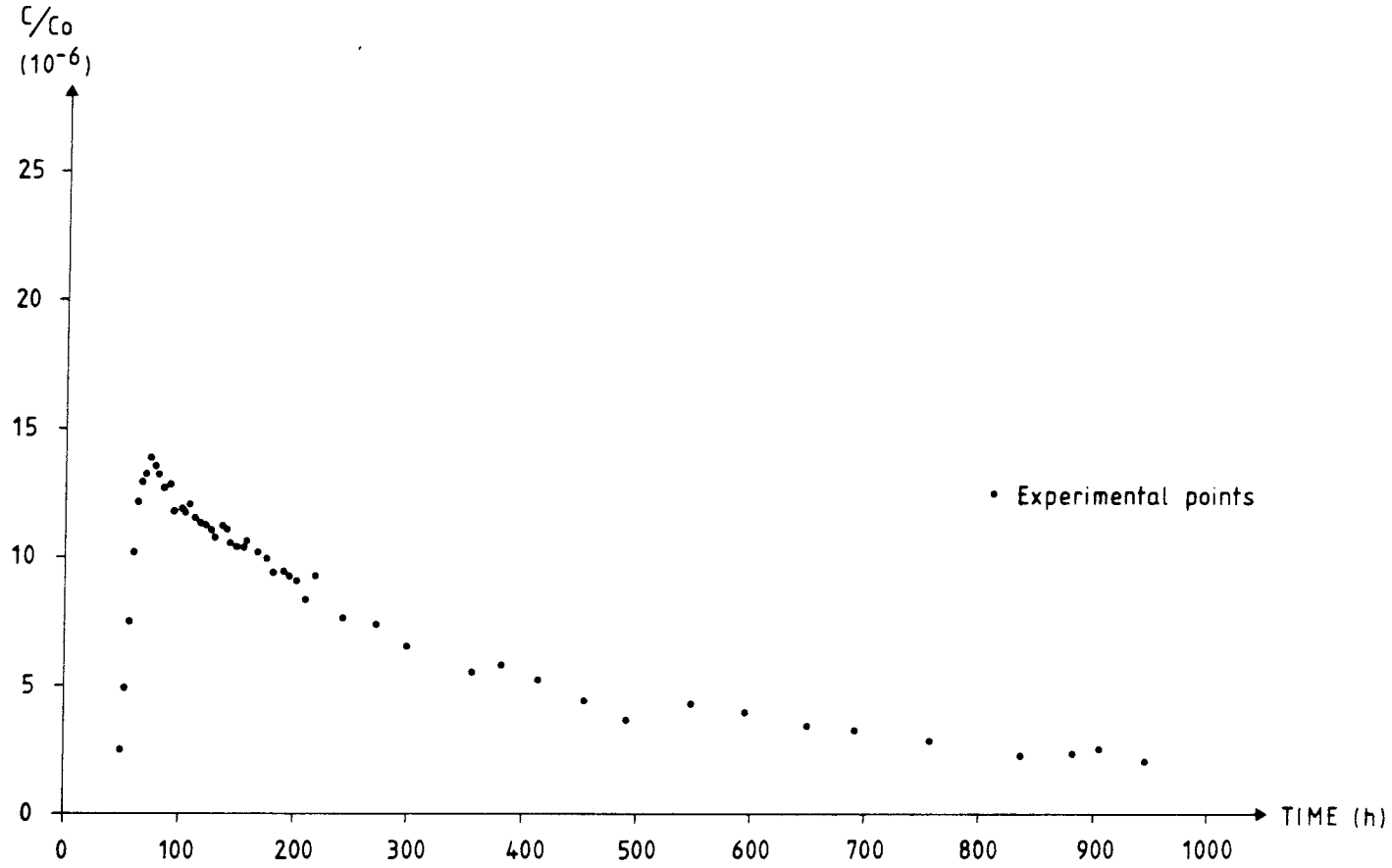

Fig. 6.3d Breakthrough curve for I-131 in test C.

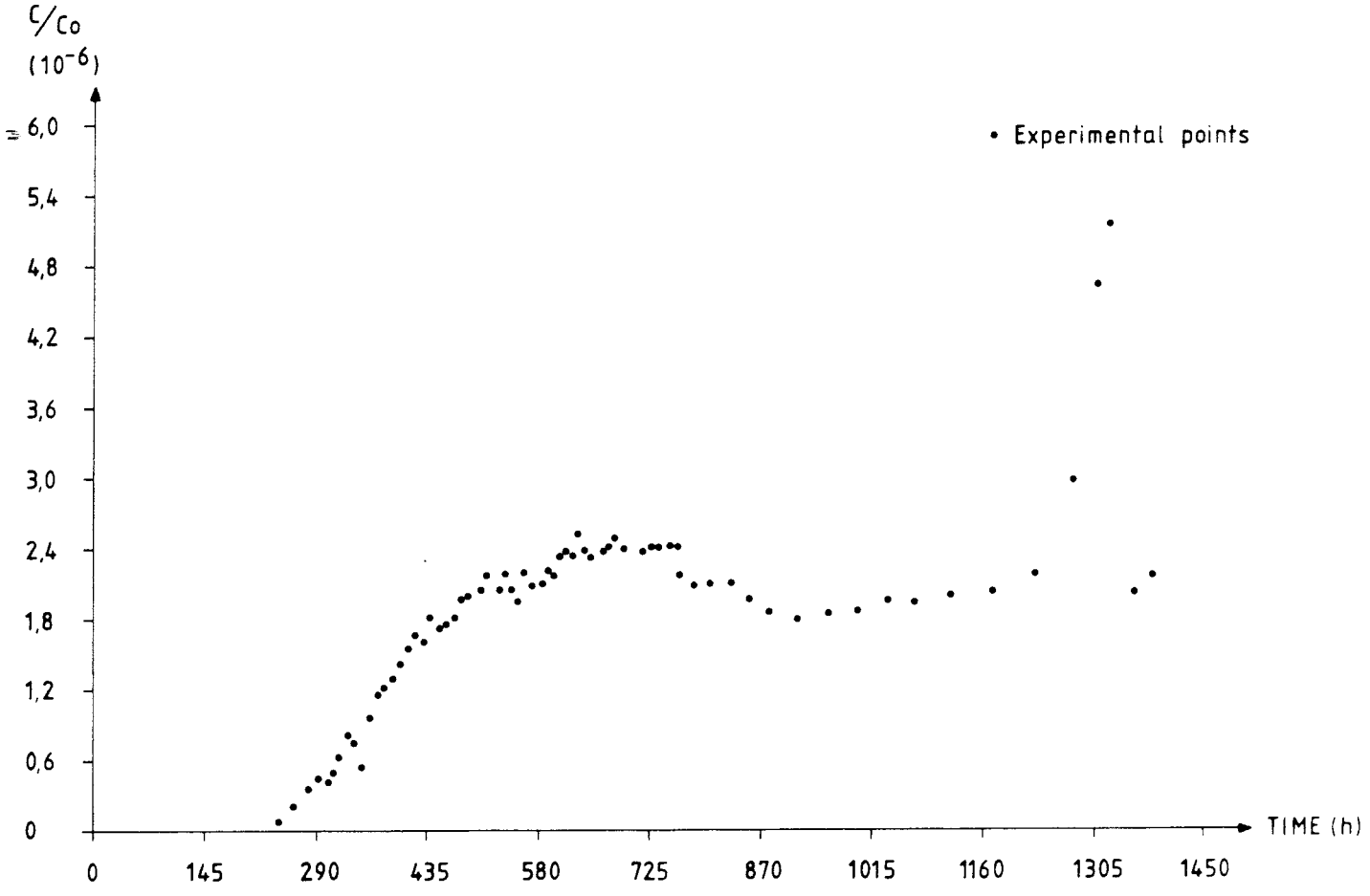

Fig. 6.3e Breakthrough curve for I-131 in test D.

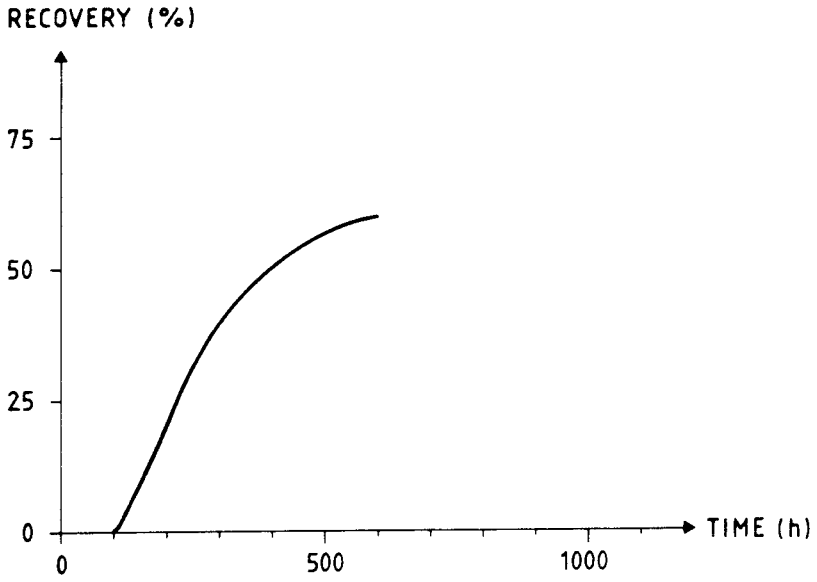

Fig. 6.3f Recovery curve for I-131 in test A.

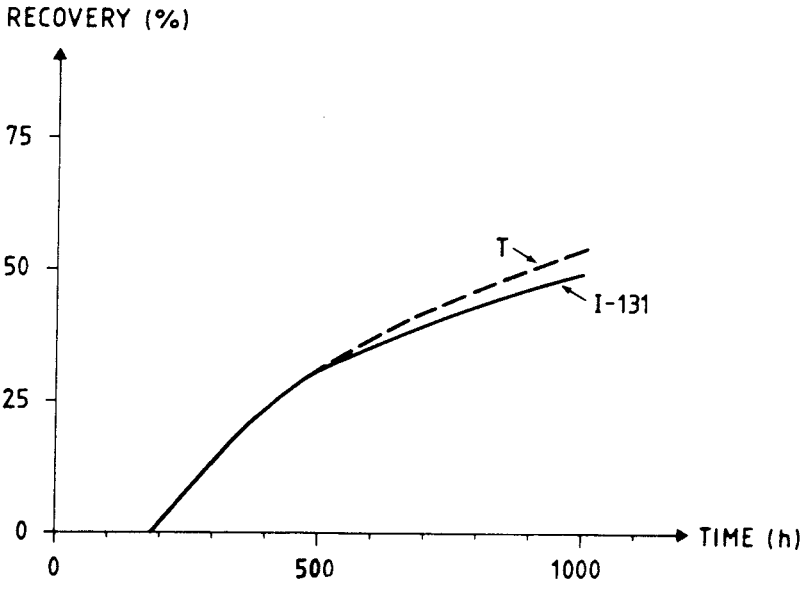

Fig. 6.3g Recovery curves for I-131 and T in test B.

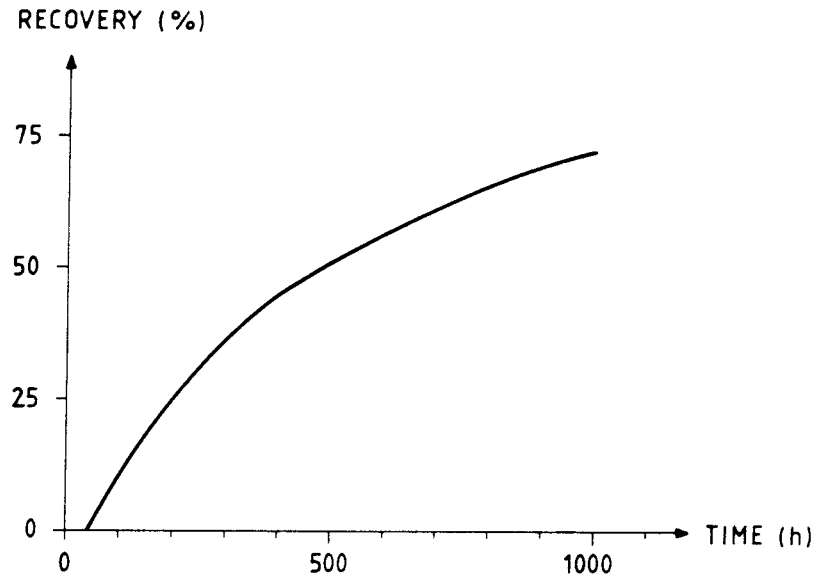

Fig. 6.3h Recovery curve for I-131 in test C.

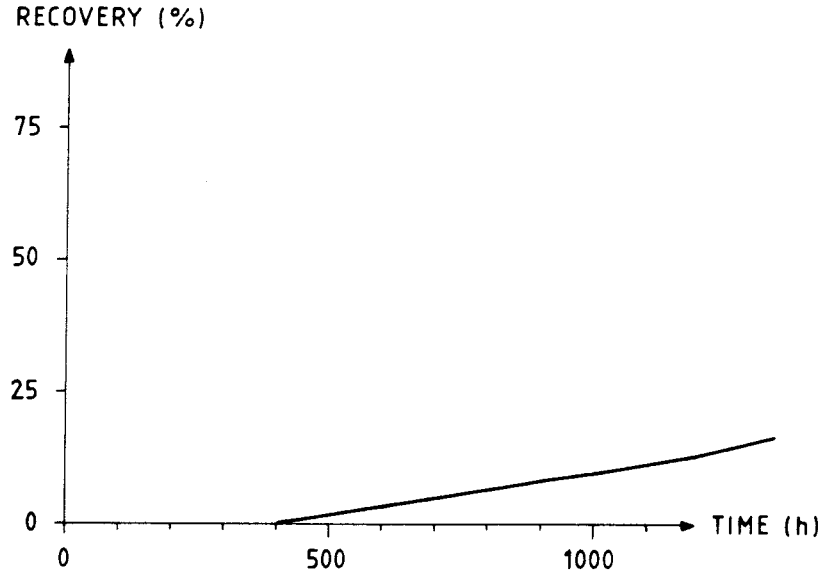

Fig. 6.3i Recovery curve for I-131 in test D.

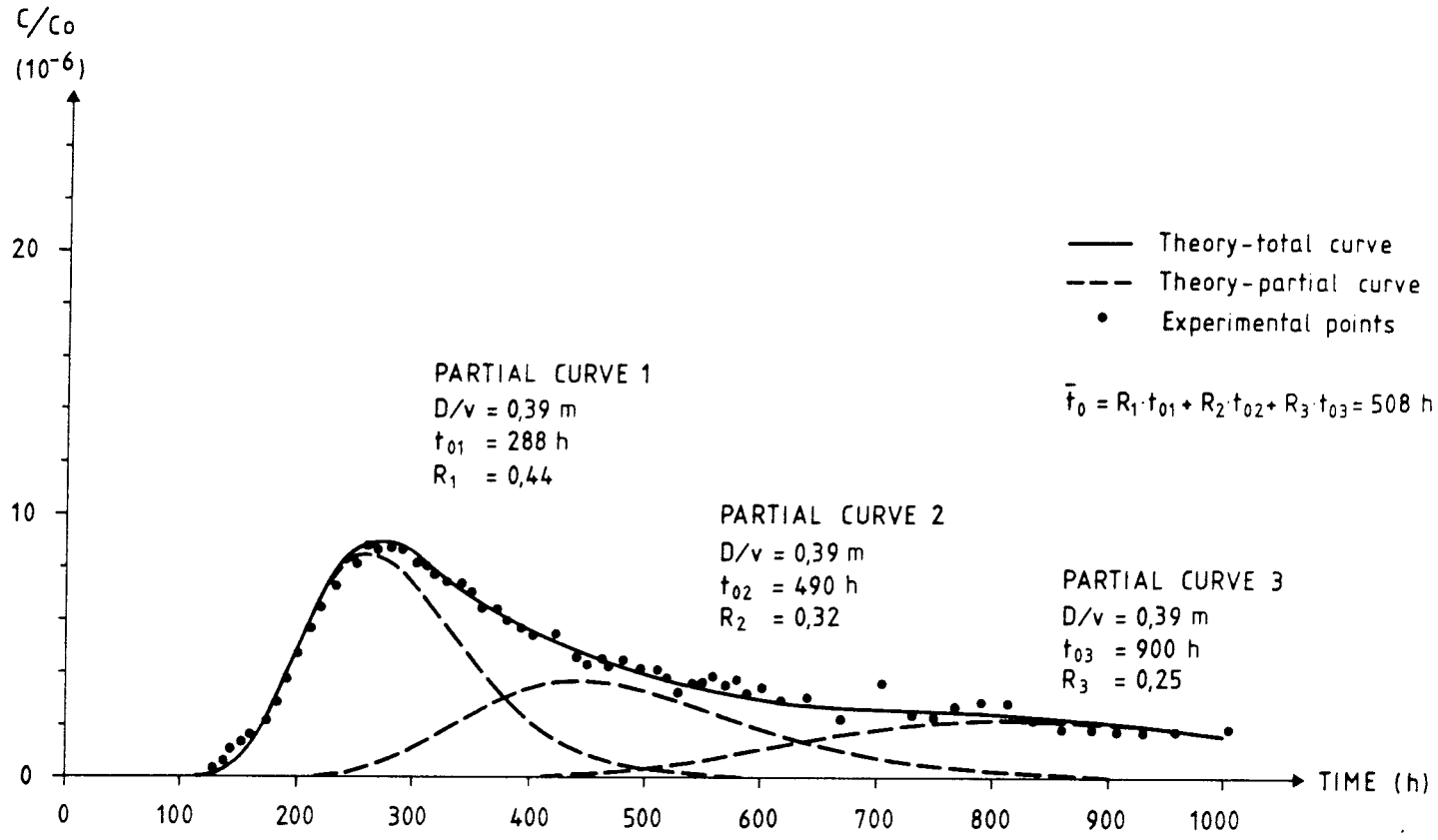

Fig. 6.4a Experimental breakthrough curve for I-131 in test B and fitting attempt B1 to theoretical model.

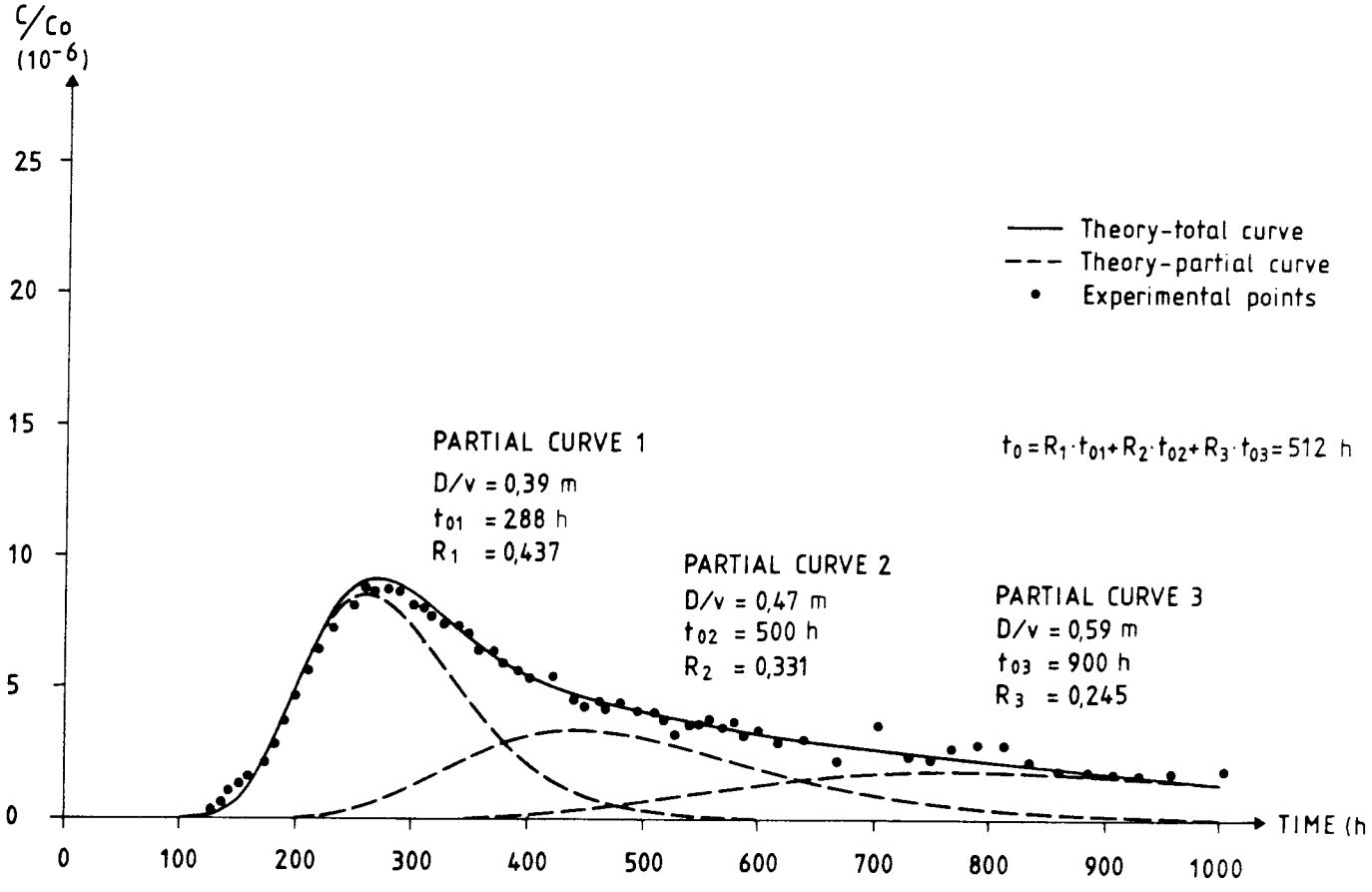

Fig. 6.4b Experimental breakthrough curve for I-131 in test B and fitting attempt B2 to theoretical model.

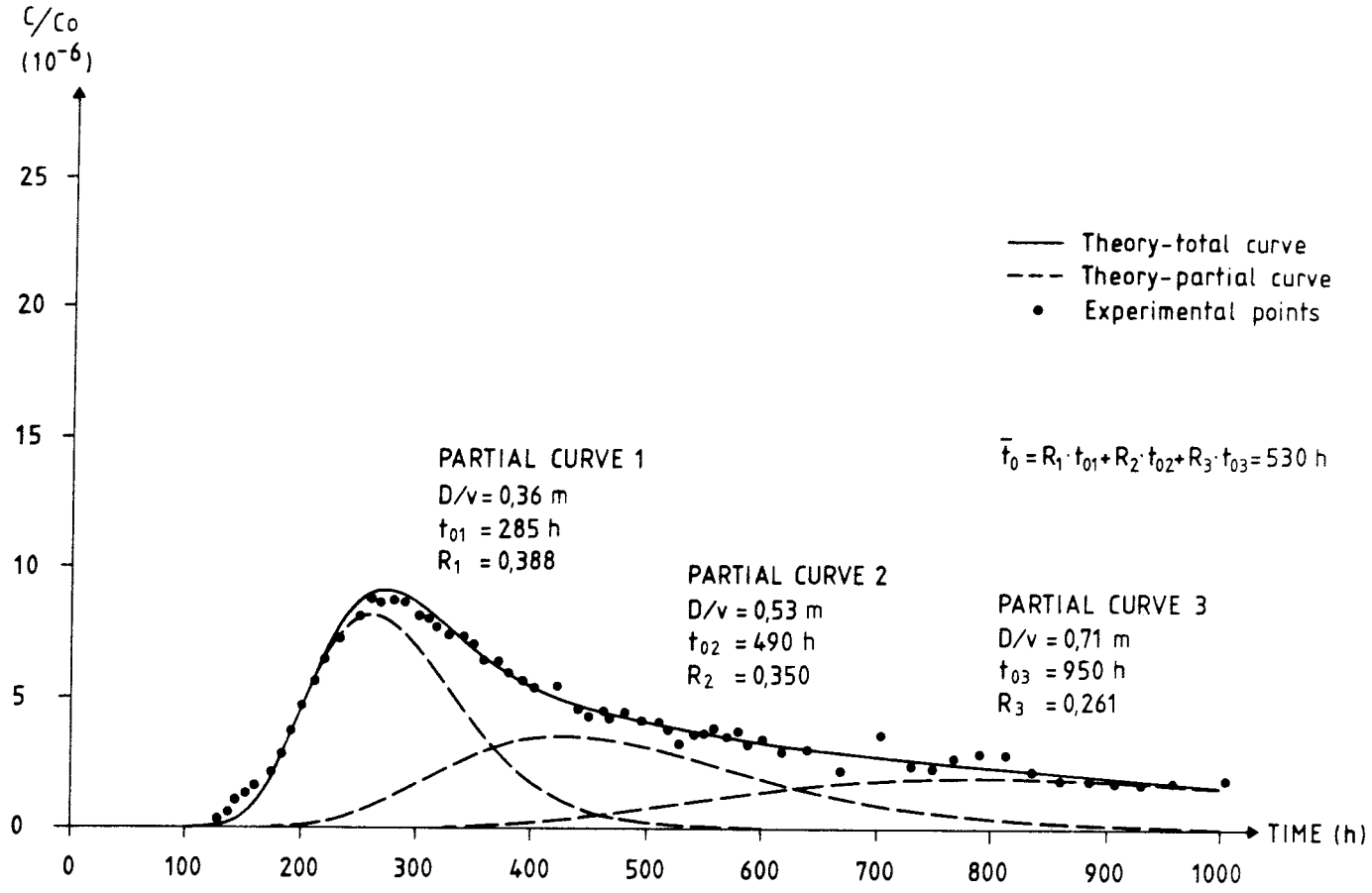

Fig. 6.4c Experimental breakthrough curve for I-131 in test B and fitting attempt B3 to theoretical model.

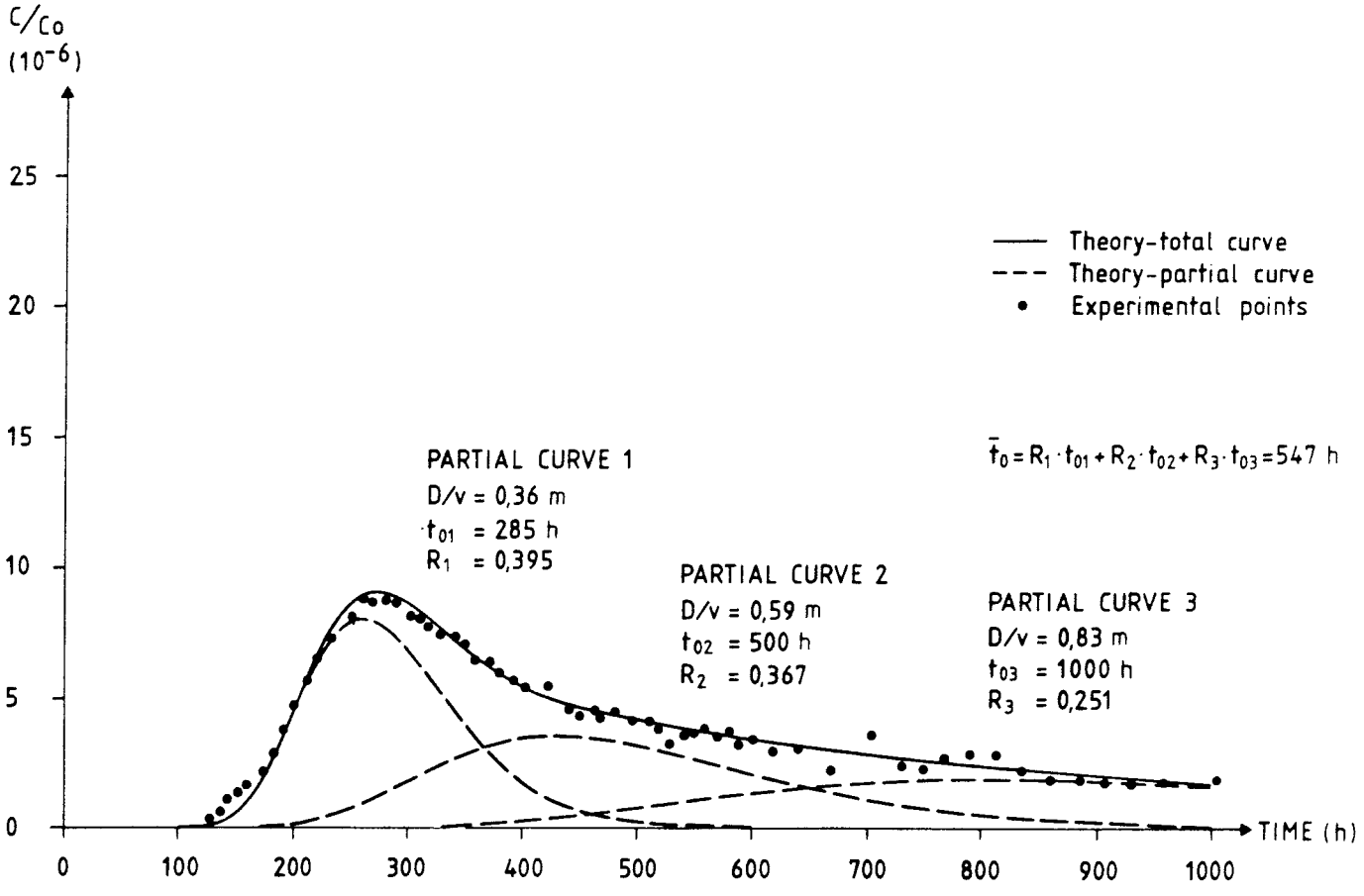

Fig. 6.4d Experimental breakthrough curve for I-131 in test B and fitting attempt B4 to theoretical model.

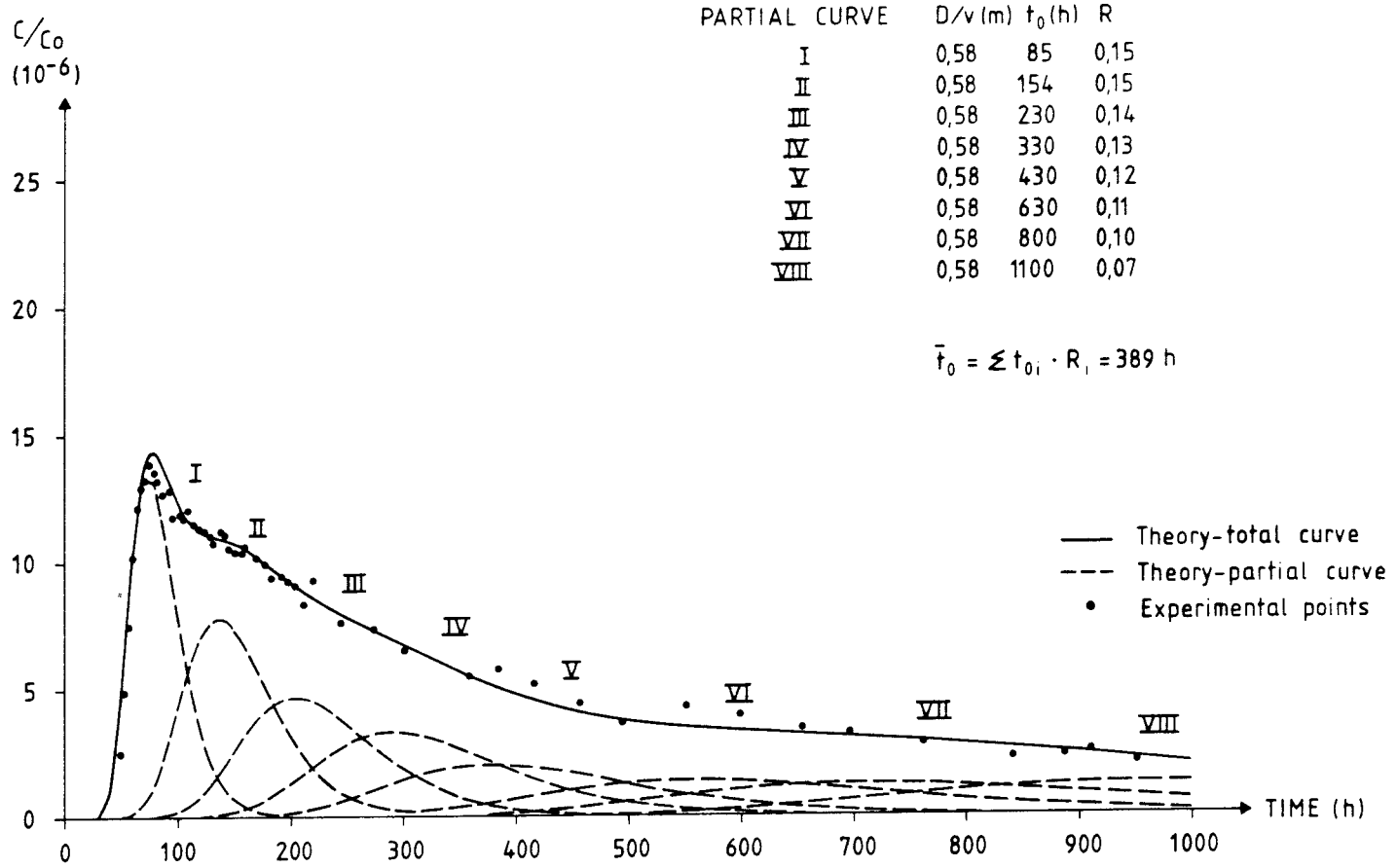

Fig. 6.4e Experimental breakthrough curve for I-131 in test C and fitting attempt C1 to theoretical model.

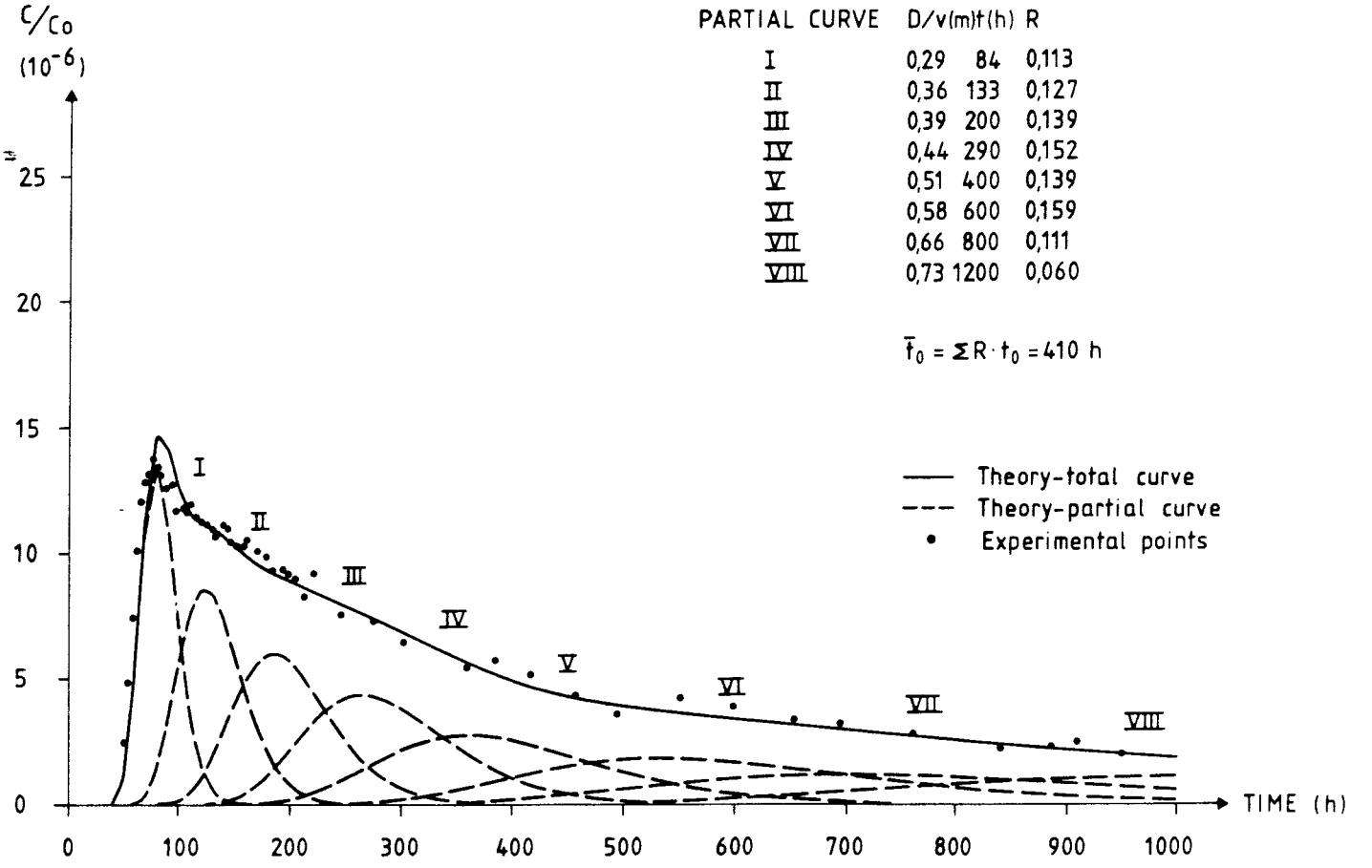

Fig. 6.4f Experimental breakthrough curve for I-131 in test C and fitting attempt C2 to theoretical model.

FÖRTECKNING ÖVER KBS TEKNISKA RAPPORTER

1977-78

TR 121 KBS Technical Reports 1 - 120.
Summaries. Stockholm, May 1979.

1979

TR 79-28 The KBS Annual Report 1979.
KBS Technical Reports 79-01--79-27.
Summaries. Stockholm, March 1980.

1980

TR 80-26 The KBS Annual Report 1980.
KBS Technical Reports 80-01--80-25.
Summaries. Stockholm, March 1981.

1981

TR 81-17 The KBS Annual Report 1981.
KBS Technical Reports 81-01--81-16
Summaries. Stockholm, April 1982.

1982

TR 82-01 Hydrothermal conditions around a radioactive waste repository
Part 3 - Numerical solutions for anisotropy
Roger Thunvik
Royal Institute of Technology, Stockholm, Sweden
Carol Braester
Institute of Technology, Haifa, Israel
December 1981

TR 82-02 Radiolysis of groundwater from HLW stored in copper canisters
Hilbert Christensen
Erling Bjergbakke
Studsvik Energiteknik AB, 1982-06-29

TR 82-03 Migration of radionuclides in fissured rock:
Some calculated results obtained from a model based on the concept of stratified flow and matrix diffusion
Ivars Neretnieks
Royal Institute of Technology
Department of Chemical Engineering
Stockholm, Sweden, October 1981

TR 82-04 Radionuclide chain migration in fissured rock -
The influence of matrix diffusion
Anders Rasmuson *
Akke Bengtsson **
Bertil Grundfelt **
Ivars Neretnieks *
April, 1982

* Royal Institute of Technology
Department of Chemical Engineering
Stockholm, Sweden

** KEMAKTA Consultant Company
Stockholm, Sweden

TR 82-05 Migration of radionuclides in fissured rock -
Results obtained from a model based on the concepts of hydrodynamic dispersion and matrix diffusion
Anders Rasmuson
Ivars Neretnieks
Royal Institute of Technology
Department of Chemical Engineering
Stockholm, Sweden, May 1982

TR 82-06 Numerical simulation of double packer tests
Calculation of rock permeability
Carol Braester
Israel Institute of Technology, Haifa, Israel
Roger Thunvik
Royal Institute of Technology
Stockholm, Sweden, June 1982

TR 82-07 Copper/bentonite interaction
Roland Pusch
Division Soil Mechanics, University of Luleå
Luleå, Sweden, 1982-06-30

TR 82-08 Diffusion in the matrix of granitic rock
Field test in the Stripa mine
Part 1
Lars Birgersson
Ivars Neretnieks
Royal Institute of Technology
Department of Chemical Engineering
Stockholm, Sweden, July 1982

TR 82-09:1 Radioactive waste management plan
PLAN 82
Part 1 General
Stockholm, June 1982

TR 82-09:2 Radioactive waste management plan
PLAN 82
Part 2 Facilities and costs
Stockholm, June 1982

TR 82-10 The hydraulic properties of fracture zones and tracer tests with non-reactive elements in Studsvik
Carl-Erik Klockars
Ove Persson
Geological Survey of Sweden, Uppsala
Ove Landström, Studsvik Energiteknik, Nyköping
Sweden, April 1982

TR 82-11 Radiation levels and absorbed doses around copper canisters containing spent LWR fuel
Klas Lundgren
Västerås, Sweden, 1982-08-11